

# A Chiral Quadruple-Stranded Helicate Cage for Enantioselective Recognition and Separation

Weimin Xuan, Mengni Zhang, Yan Liu, Zhijie Chen, and Yong Cui\*

School of Chemistry and Chemical Technology and State Key Laboratory of Metal Matrix Composites, Shanghai Jiao Tong University, Shanghai 200240, China

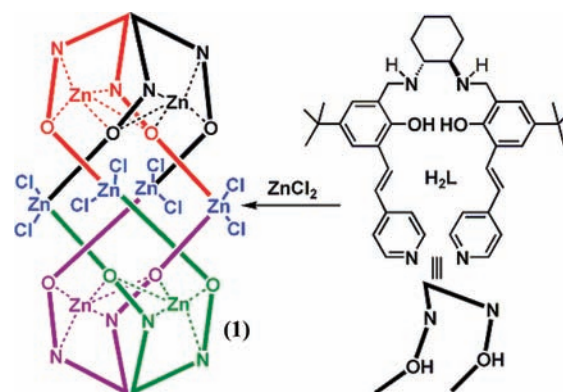
**S** Supporting Information

**ABSTRACT:** The self-assembly of enantiopure pyridyl-functionalized metallosalan units affords a homochiral helicate cage,  $[Zn_8L_4Cl_8]$ , in which the optical rotation of each ligand is increased by a factor of 10 upon coordination. The octanuclear cage featuring a chiral amphiphilic cavity exhibits enantioselective luminescence enhancement by amino acids in solution. The cage exists in two different crystalline polymorphic forms that possess porous structures built of helicate cages interconnected by 1D channels or pentahedral cages and have the ability to separate small racemic molecules by adsorption but with different enantioselectivities.

Since chiral recognition is one of the fundamental processes in nature and plays vital roles in diverse fields of science and technology, many efforts have been devoted to the synthesis and utilization of artificial chiral architectures.<sup>1</sup> In particular, metal-directed self-assembly opens up unique opportunities to make well-defined coordination structures and has led to great progress in the construction of functional porous cages.<sup>2,3</sup> Incorporating chiral functional groups into such hollow structures means that they can be used for enantioselective processes,<sup>4,5</sup> but there is still difficulty in making chiral molecular cages that are optically pure.<sup>4–6</sup> In fact, with a few notable exceptions, chiral molecular coordination architectures have not been explored for enantioselectivities.<sup>6</sup>

Although helicates constructed from flexible oligodentate strands and metal ions have long attracted chemists with their elegant morphologies and intrinsic chirality,<sup>7</sup> helicate cages that have available inner cavities are very rare, and none to date have been reported to be optically pure.<sup>7,8</sup> Meanwhile, chiral salen ligands and their metal complexes have diverse applications in asymmetric catalysis and separation.<sup>9</sup> In contrast, salen ligands, the reduced forms of salen ligands, are less studied, but potential benefits such as increased ligand flexibility and stronger nitrogen donors make them attractive ligand targets.<sup>10</sup> Realizing that the salen ligand might establish a pair of unique asymmetric NH recognition sites,<sup>1b</sup> we examined the coordination assembly of twisted enantiopure metallosalans for creating chiral helical cavities and functionalities for chirotechnology. We report here the assembly of a homochiral helicate cage from the pyridyl-functionalized salen ligand  $H_2L$  and  $ZnCl_2$  (Scheme 1). The cage exhibits enantioselective luminescence enhancement by chiral amino acids, and its

Scheme 1. Assembly of Helicate Cage 1 from  $H_2L$



crystalline samples can serve as hosts for adsorption separation of racemic organic molecules.

The chiral salen ligand  $H_2L$  was prepared in an overall 56% yield by the Schiff base condensation of 5-*tert*-butyl-3-(4-vinylpyridyl)salicylaldehyde and enantiopure 1,2-diaminocyclohexane followed by reduction with  $NaBH_4$ . Reaction of (*R*)- $H_2L$  with  $ZnCl_2$  (1:2 molar ratio) in a mixed solvent of DMF, THF, and  $H_2O$  by slow evaporation at room temperature or by heating at 65 °C afforded complexes  $[Zn_8L_4Cl_8] \cdot 5THF$  [(*R*)-**1a**] or  $[Zn_8L_4Cl_8] \cdot THF \cdot H_2O$  [(*R*)-**1b**] in good yields. The formulations were supported by the results of microanalysis, IR spectroscopy, and thermogravimetric analysis (TGA). The solution behaviors of **1a** and **1b** are essentially the same, so only that of the former will be presented.

The  $^1H$  NMR spectrum of (*R*)-**1a** shows more complicated signals than the free  $H_2L$  ligand (Figure 1). First, there is one complete set of proton resonances for the L ligand, as could be deduced from the number of signals and the appearance of two sets of signals for the *tert*-butyl groups at 1.12 and 1.25 ppm. This indicates that the  $C_2$  symmetry of the ligand is lost in the cage complex. Second, with respect to the free ligand, the proton signals from the cyclohexane groups show an obvious upfield shift, while those from the pyridyl and phenyl groups show either downfield or upfield shifts, suggesting the unsymmetrical coordination behavior of the ligand. Finally, all of the proton signals are very sharp, suggesting the formation of discrete metal complexes rather than oligomeric species. The formation of the cage compound was supported by electrospray

Received: December 28, 2011

Published: April 11, 2012

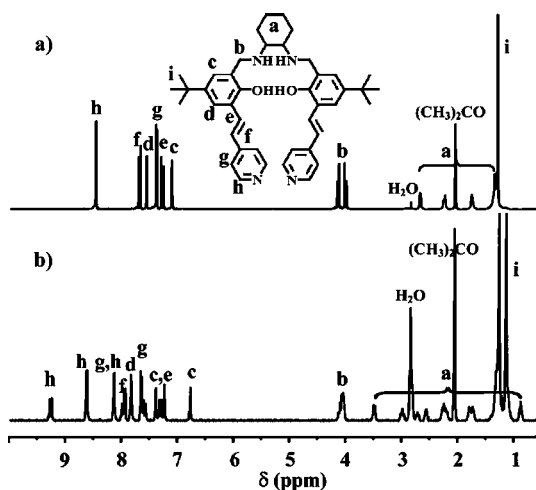


**Figure 1.**  $^1\text{H}$  NMR spectra of (a)  $(R)\text{-H}_2\text{L}$  and (b)  $(R)\text{-1a}$  in acetone- $d_6$ .

ionization mass spectrometry (ESI-MS) of  $(R)\text{-1a}$ , which showed the molecular ion  $[\text{Zn}_8\text{L}_4\text{Cl}_7]^+$  at  $m/z$  3325.1 and the fragment ions  $[\text{Zn}_4\text{L}_4 + \text{Na} + 3\text{H}]^{4+}$ ,  $[\text{Zn}_2\text{L}_2 + \text{NH}_4]^+$ , and  $[\text{Zn}_4\text{L}_4 + \text{K}]^+$  at  $m/z$  713.5, 1431.3, and 2865.0, respectively (Figure S16 in the Supporting Information).

A single-crystal X-ray diffraction (XRD) study of  $(R)\text{-1a}$  unambiguously revealed the formation of a chiral helicate cage.  $(R)\text{-1a}$  crystallizes in the chiral monoclinic  $P2_1$  space group, with one formula unit in the asymmetric unit. The basic building unit is a  $\text{Zn}_2\text{L}_2$  dimer built of  $\text{ZnL}$  monomers (Figure 2a). The dimetallic core consists of two five-coordinate

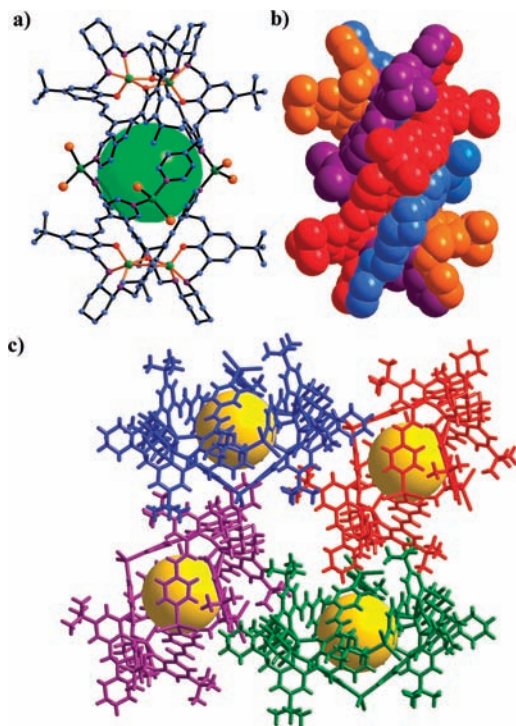


**Figure 2.** (a) View of the molecular structure of  $(R)\text{-1a}$  (dark-green, Zn; yellow, Cl; blue, C; red, O; purple, N) and (b) its space-filling model. (c) The 3D supramolecular structure of  $(R)\text{-1a}$  showing helicate cages interconnected by channels. The cavities are highlighted by colored spheres.

trigonal-bipyramidal Zn centers enclosed in the  $\text{N}_2\text{O}_2$  pockets and linked by two phenolato O atoms. The dimeric unit is therefore based on two identical coordination bonds forming a four-membered  $\text{Zn}_2\text{O}_2$  ring with a Zn1–Zn2 separation of 3.0725(7) Å. The two twisted salan ligands have an antiparallel orientation around the dimetallic core, and the four pyridyl groups are oriented toward the same face of the almost planar  $\text{Zn}_2\text{O}_2$  unit and point away from the adjacent units with a separation distance of 6.8 Å (average N...N distance) to minimize steric repulsion. A pair of the bowl-like  $\text{Zn}_2\text{L}_2$  dimers are linked together via their peripheral pyridyl groups by coordination to four Zn centers in the equatorial plane. Each of the four Zn ions is tetrahedrally coordinated by two pyridyl groups and two chloride ions. Overall, the octanuclear cage can be viewed as a  $P$ -configured quadruple-stranded helicate that is locked by the twisted  $\text{Zn}_2\text{L}_2$  dimers at both ends, which take a screwed U shape and are fixed by coordination to the four  $\text{ZnCl}_2$  units.

**1b** crystallizes in the chiral orthorhombic  $P2_12_12_1$  space group, with one formula unit in the asymmetric unit. It is a polymorph of  $(R)\text{-1a}$  and has a similar  $P$ -configured helicate structure assembled from  $\text{Zn}_2\text{L}_2$  dimers. Space-filling representations of **1a** (Figure 2b) and **1b** clearly show the formation of porous helicate cages with wide apertures. The cavities have inner dimensions of  $\sim 13.7 \text{ \AA} \times 6.4 \text{ \AA}$  occupied by one THF molecule. Strong intermolecular  $\pi$ – $\pi$ ,  $\text{CH}\cdots\pi$ , and  $\text{CH}\cdots\text{Cl}$  interactions direct the packing of the helicates into porous 3D structures. In **1a**, 1D channels with dimensions of  $\sim 4.0 \text{ \AA} \times 5.5 \text{ \AA}$  are formed by stacking of adjacent tetramers along the  $[100]$  directions (Figure 2c), whereas in **1b**, distorted pentahedral cages with a maximum inner width of  $\sim 8 \text{ \AA}$  are formed via the arrangement of four adjacent helicate cages (Figure S5b). In both cases, the chiral coordinated amines of the **L** ligands are oriented toward the outside of the helicate cages and are exposed to the interstitial pores accessible to guest molecules. Compounds of this type thus have great potential for studies of host–guest interactions and supramolecular chemistry. **1a** and **1b** are rare examples of homochiral coordination cages with built-in chiral functional groups that have been crystallographically characterized.<sup>4–6</sup>

The homochiral nature of the salan ligand  $\text{H}_2\text{L}$  is essential for the formation of the helicate cage. Under otherwise identical conditions, slow evaporation of *rac*- $\text{H}_2\text{L}$  and  $\text{ZnCl}_2$  in the DMF/THF/ $\text{H}_2\text{O}$  mixed solvent afforded only a racemic dimeric complex  $[\text{Zn}_2\text{L}_2]$  (**2**) instead of the expected helicate complex. In **2**, the dinuclear unit is built of two opposite-handed ligands in which the four pyridyl groups are oriented toward the different faces of the almost planar  $\text{Zn}_2\text{O}_2$  core, thus disfavoring the generation of a helicate coordination structure as a result of spatial constraints (Figure S7). Calculations using the PLATON program indicate that 40.9 and 51.1% of the total volumes of **1a** and **1b**, respectively, are occupied by solvent molecules.<sup>11</sup> The phase purity of bulk samples of **1a** and **1b** was established by comparison of their observed and simulated powder XRD (PXRD) patterns. TGA revealed that guest molecules could be removed at 80–150 °C. PXRD indicated that the evacuated samples retained their crystallinity, although structural distortions occurred. The apohost structure took up guest molecules again upon exposure to THF vapor for 2 days at room temperature, as evidenced by TGA and PXRD. The permanent porosity of **1a** and **1b** was examined by  $\text{N}_2$  adsorption measurements at 77 K, and the BET surface areas were found to be 78.0 and 283.7  $\text{m}^2/\text{g}$ , respectively.

Chiral amplification occurred during the self-assembly of the enantiopure helicate. The values of the molar optical rotation ( $\phi$ ) of (*R*)-**1a** and  $H_2L$  are 31208.7 and 674.9 deg cm<sup>3</sup> dm<sup>-1</sup> mol<sup>-1</sup>, respectively. The cage bearing four ligands has an optical rotation per mole that is >45 times that of  $H_2L$ , that is, a 10-fold increase in optical rotation between a set of four free ligands and a set of four coordinated ligands. The generation of a chiral helical superstructure should be responsible for the 10-fold increase of the optical rotation. This molar optical rotation value is large in absolute terms, comparable to those of organic helicenes<sup>12a</sup> and the resolved trefoil knot.<sup>12b</sup> The solution CD spectra of **1a** made from (*S*)- and (*R*)- $H_2L$  are mirror images of each other, and each exhibited a bisignate  $\pi$ - $\pi^*$  band at 274 and 371 nm. Their intensities are much higher than that of the free ligand, consistent with the molar optical result. The solid-state CD spectra showed their enantiopurity and retention of chirality in the crystalline state.

The presence of large chiral pores and available chiral functional NH groups in this helicate cage prompted the exploration of enantioselective recognition and separation. The fluorescence of cage (*R*)-**1a** in THF showed a strong emission at  $\lambda = 534$  nm assigned to a ligand-centered  $\pi \rightarrow \pi^*$  process, with a quantum yield of 5.60% and lifetimes of 2.31 and 0.92 ns (corresponding to a biexponential decay). When (*R*)-**1a** was treated with Ala, the emission at 534 nm was shifted to 515 nm and enhanced by both the *D* and *L* enantiomers (Figure 3), but

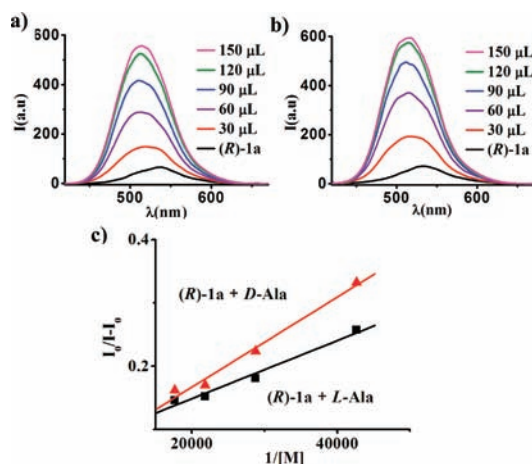


**Figure 3.** Fluorescence enhancement of (*R*)-**1a** ( $1.0 \times 10^{-5}$  M in THF) upon titration with (a) *D*-Ala ( $1 \times 10^{-3}$  M) and (b) *L*-Ala ( $1 \times 10^{-3}$  M) and (c) the Benesi–Hildebrand plot.

the increase caused by *L*-Ala was greater than that by *D*-Ala, implying enantioselectivity in the fluorescence recognition. The fluorescence intensity of **1a** was maximally increased to 7.6 and 7.0 times that of the original value by *L*- and *D*-Ala, respectively. Figure 3c shows Benesi–Hildebrand plots for (*R*)-**1a** ( $1.0 \times 10^{-5}$  M) in the presence of *L*- and *D*-Ala in THF. The association constants  $K_{BH}$  were found to be 12363 M<sup>-1</sup> with *L*-Ala and 3352 M<sup>-1</sup> with *D*-Ala, giving an enantioselectivity factor  $K_{BH}(R-L)/K_{BH}(R-D)$  of 3.69. The opposite trend in enantioselectivity was observed for the enhancement of (*S*)-**1a** by Ala, for which the enantioselectivity factor  $K_{BH}(S-D)/K_{BH}(S-L)$  was 3.57, further confirming a chirality-based luminescence-enhancing selectivity. Notably, the free ligand  $H_2L$  showed no obvious enantioselectivity, suggesting that the helical structure confers a better-defined chiral environment.<sup>13</sup> After titration, the quantum yield of (*R*)-**1a** increased from 5.60

to 29.1% and the biexponential fluorescence lifetimes changed slightly to 1.93 and 0.91 ns, respectively.

The observed change in the fluorescence intensity of **1a** is probably a result of static enhancement by the formation of a hydrogen-bonded cage–amino acid adduct that may induce changes in the structure of the emitting species, such as a change and/or rigidification of the conformation and excimer formation.<sup>13,14</sup> The static complexation is suggested by the nearly stable fluorescence lifetimes of **1a** before and after titration. Because the noncovalent interactions of **1a** with amino acid enantiomers generate different diastereomeric complexes, a distinct fluorescence enhancement is detected. The formation of a stable adduct complex between (*R*)-**1a** and *L*-Ala is supported by ESI-MS, which showed five prominent peaks at  $m/z$  903.0, 993.4, 1085.8, 1173.5, and 1264.0, corresponding to  $[Zn_8L_4Cl_5 + 4L-Ala + H]^+$ ,  $[Zn_8L_4Cl_5 + 8L-Ala + H]^+$ ,  $[Zn_8L_4Cl_5]^{3+}$ ,  $[Zn_8L_4Cl_5 + 3L-Ala]^{3+}$ , and  $[Zn_8L_4Cl_5 + 6L-Ala]^{3+}$ , respectively. <sup>1</sup>H NMR analysis also suggested the complexation of **1a** and Ala (Figure S28).

Other chiral amino acids such as Phe and Val were also found to enhance the fluorescence of (*R*)-**1a** but gave lower enantioselectivity than Ala, probably because the steric hindrance of bulky phenyl groups impaired the chiral recognition ability. It is interesting to note that very weak enantioselectivity was observed for the luminescence enhancement of (*R*)-**1a** by the *N*-Boc-protected amino acid *N*-Boc-Ala, which supports the involvement of amino groups in the formation of a ground-state hydrogen-bonded complex and an excited-state proton-transfer complex. Many synthetic receptors for chiral recognition of amino acids have been synthesized; however, no assembled helicates or cages have been reported to exhibit such enantioselectivity.<sup>1c,15,7</sup>

The separation capabilities of the crystalline cages toward 1-(methylsulfinyl)benzene, 1-phenylethanol, 1-phenylpropanol, and 1-phenylethylamine were evaluated by immersing the apohost samples in diethyl ether solutions of the racemic adsorbates. Chiral HPLC analyses of the four guests from (*R*)-**1a** desorbed yielded 20.1, 4.7, 13.0 and 14.6% ee, respectively, with the *S* enantiomers being in excess. Compared with (*R*)-**1a**, (*R*)-**1b** exhibited enhanced enantioselectivities for (*S*)-1-(methylsulfinyl)benzene (37.5% ee), (*S*)-1-phenylethanol (13.8% ee), and (*S*)-1-phenylpropanol (18.6% ee) but a decreased enantioselectivity for (*S*)-1-phenylethylamine (10.3% ee). Their different recognition enantioselectivities may be due to their different porous structures, in which **1a** is built of helicate cages interconnected by channels whereas **1b** is built of helicate cages interconnected by pentahedral cages. Neither adsorbent could take up larger substrates such as 1-(1-naphthyl)ethanol and 1-(1-naphthyl)ethylamine because of their small channels. Control experiments showed that the  $H_2L$  ligand itself could not resolve the enantiomers of the examined substrates under otherwise identical conditions, indicating that the well-organized structure of the chiral centers of the metallosalan units controls the enantioselective recognition process. The adsorbents could be regenerated after adsorption and reused without performance loss. For example, the second and third recycled samples of **1b** provided 31.0 and 32.5% ee, respectively, for separating racemic 1-(methylsulfinyl)benzene. PXRD showed that the recycled sample retained crystallinity after three runs but that the structure became seriously distorted. Alternatively, the crystalline samples could easily be recycled by recrystallization from THF at room temperature or 65 °C. The supramolecular engineering of permanent porous

solids from intrinsically porous cages is of significance but remains challenging.<sup>6b</sup> Despite the limited enantioselectivity, the present crystalline cage materials represent a new generation of chiral porous solids that are capable of chiral separation of different types of molecules simultaneously.<sup>5f,16</sup> Further studies on separating other racemic compounds and understanding the enantioselective processes are underway.

In conclusion, we have presented the assembly of homochiral quadruple-stranded helicate cages from metallosalans and demonstrated their enantioselective abilities to recognize enantiomers of amino acids via fluorescence enhancement in solution and to separate small racemic organic molecules by adsorption in the crystalline state. The readily tunability of such a modular approach based on metallosalan units promises to lead a number of chiral assemblies with unique and practically useful enantioselective functions.

## ■ ASSOCIATED CONTENT

### Supporting Information

Experimental procedures and characterization data. This material is available free of charge via the Internet at <http://pubs.acs.org>.

## ■ AUTHOR INFORMATION

### Corresponding Author

yongcui@sju.edu.cn.

### Notes

The authors declare no competing financial interest.

## ■ ACKNOWLEDGMENTS

This work was supported by the NSFC (21025103 and 20971085), the "973" Program (2009CB930403), and the Shanghai Science and Technology Committee (10DJ1400100).

## ■ REFERENCES

- (1) (a) Hof, F.; Craig, S. L.; Nuckolls, C.; Rebek, J., Jr. *Angew. Chem. Int. Ed.* **2002**, *41*, 1488. (b) Moberg, C. *Angew. Chem., Int. Ed.* **2006**, *45*, 4721. (c) Pu, L. *Acc. Chem. Res.* **2012**, *45*, 150.
- (2) (a) Chakrabarty, R.; Mukherjee, P. S.; Stang, P. J. *Chem. Rev.* **2011**, *111*, 6810. (b) Fujita, M.; Tominaga, M.; Hori, A.; Therrien, B. *Acc. Chem. Res.* **2005**, *38*, 369. (c) Ward, M. D. *Chem. Commun.* **2009**, 4487. (d) Pluth, M. D.; Bergman, R. G.; Raymond, K. N. *Acc. Chem. Res.* **2009**, *42*, 1650. (e) Koblenz, T. S.; Wassenaar, J.; Reek, J. N. H. *Chem. Soc. Rev.* **2008**, *37*, 247. (f) Saalfrank, R. W.; Maid, H.; Scheurer, A. *Angew. Chem., Int. Ed.* **2008**, *47*, 8794. (g) Pascu, G. I.; Hotze, A. C. G.; Sanchez-Cano, C.; Kariuki, B. M.; Hannon, M. J. *Angew. Chem., Int. Ed.* **2007**, *46*, 4374. (h) Hotze, A. C. G.; Kariuki, B. M.; Hannon, M. J. *Angew. Chem., Int. Ed.* **2006**, *45*, 4839. (i) Allen, K.; Faulkner, R.; Harding, L.; Rice, C.; Riis-Johannessen, T.; Voss, M.; Whitehead, M. *Angew. Chem., Int. Ed.* **2010**, *49*, 6655. (j) Jeffery, J.; Rice, C.; Harding, L.; Baylies, C.; Riis-Johannessen, T. *Chem.—Eur. J.* **2007**, *13*, 5256.
- (3) (a) Pluth, M. D.; Bergman, R. G.; Raymond, K. N. *Science* **2007**, *316*, 85. (b) Mal, P.; Breiner, B.; Rissanen, K.; Nitschke, J. R. *Science* **2009**, *324*, 1697. (c) Kuil, M.; Soltner, T.; Van Leeuwen, P. W. N. M.; Reek, J. N. H. *J. Am. Chem. Soc.* **2006**, *128*, 11344. (d) Sun, Q.; Iwasa, J.; Ogawa, D.; Ishido, Y.; Sato, S.; Ozeki, T.; Sei, Y.; Yamaguchi, K.; Fujita, M. *Science* **2010**, *328*, 1144. (e) Ito, H.; Ikeda, M.; Hasegawa, T.; Furusho, Y.; Yashima, E. *J. Am. Chem. Soc.* **2011**, *133*, 3419. (f) Yashima, E.; Maeda, K.; Furusho, Y. *Acc. Chem. Res.* **2008**, *41*, 1166. (g) Meng, W.; Clegg, J. K.; Thoburn, J. D.; Nitschke, J. R. *J. Am. Chem. Soc.* **2011**, *133*, 13652. (h) Ayme, J.-F.; Beves, J. E.; Leigh, D. A.; McBurney, R. T.; Rissanen, K.; Schultz, D. *Nat. Chem.* **2012**, *4*, 15.
- (4) (a) Argent, S. P.; Riis-Johannessen, T.; Jeffery, J. C.; Harding, L. P.; Ward, M. D. *Chem. Commun.* **2005**, 4647. (b) Ziegler, M.; Davis, A. V.; Johnson, D. W.; Raymond, K. N. *Angew. Chem., Int. Ed.* **2003**, *42*,

665. (c) Albrecht, M.; Burk, S.; Weis, P. *Synthesis* **2008**, 2963. (d) Hamilton, T. D.; MacGillivray, L. R. *Cryst. Growth Des.* **2004**, *4*, 419.

(5) (a) Nishioka, Y.; Yamaguchi, T.; Kawano, M.; Fujita, M. *J. Am. Chem. Soc.* **2008**, *130*, 8160. (b) Leung, D. H.; Bergman, R. G.; Raymond, K. N. *J. Am. Chem. Soc.* **2006**, *128*, 9781. (c) Nakamura, A.; Inoue, Y. *J. Am. Chem. Soc.* **2005**, *127*, 5338. (d) Davis, A. V.; Fiedler, D.; Ziegler, M.; Terpin, A.; Raymond, K. N. *J. Am. Chem. Soc.* **2007**, *129*, 15354. (e) Fiedler, D.; Leung, D. H.; Bergman, R. G.; Raymond, K. N. *J. Am. Chem. Soc.* **2004**, *126*, 3674. (f) Liu, T.; Liu, Y.; Xuan, W.; Cui, Y. *Angew. Chem., Int. Ed.* **2010**, *49*, 4121.

(6) (a) Iwasawa, T.; Hooley, R. J.; Rebek, J., Jr. *Science* **2007**, *317*, 493. (b) Holst, R.; Trewin, A.; Cooper, A. I. *Nat. Chem.* **2010**, *2*, 915. (c) Liu, X. J.; Warmuth, R. *J. Am. Chem. Soc.* **2006**, *128*, 14120. (d) Liu, Y. Z.; Hu, C. H.; Comotti, A.; Ward, M. D. *Science* **2011**, *333*, 436. (e) Icli, B.; Christinat, N.; Tonnemann, J.; Schuttler, C.; Scopelliti, R.; Severin, K. *J. Am. Chem. Soc.* **2009**, *131*, 3154. (f) Jin, Y.; Voss, B. A.; Jin, A.; Long, H.; Noble, R. D.; Zhang, W. *J. Am. Chem. Soc.* **2011**, *133*, 6650.

(7) (a) Piguet, C.; Bernardinelli, G.; Hopfgartner, G. *Chem. Rev.* **1997**, *97*, 2005. (b) Albrecht, M. *Chem. Rev.* **2001**, *101*, 3457. (c) Xi, X.; Fang, Y.; Dong, T.; Cui, Y. *Angew. Chem., Int. Ed.* **2011**, *50*, 1154. (d) Howson, S. E.; Bolhuis, A.; Brabec, V.; Clarkson, G. J.; Malina, J.; Rodger, A.; Scott, P. *Nat. Chem.* **2012**, *4*, 31.

(8) (a) Koshevoy, I. O.; Haukka, M.; Selivanov, S. I.; Tunik, S. P.; Pakkanen, T. A. *Chem. Commun.* **2010**, 46, 8926. (b) Crowley, J. D.; Gavey, E. L. *Dalton Trans.* **2010**, 39, 4035. (c) Scherer, M.; Caulder, D. L.; Johnson, D. W.; Raymond, K. N. *Angew. Chem., Int. Ed.* **1999**, *38*, 1588. (d) Caulder, D. L.; Raymond, K. N. *Angew. Chem., Int. Ed. Engl.* **1997**, *36*, 1440.

(9) (a) Baleizao, C.; Garcia, H. *Chem. Rev.* **2006**, *106*, 3987. (b) Clever, G. H.; Polborn, K.; Carell, T. *Angew. Chem., Int. Ed.* **2005**, *44*, 7204.

(10) (a) Matsumoto, K.; Saito, B.; Katsuki, T. *Chem. Commun.* **2007**, 3619. (b) Egami, H.; Oguma, T.; Katsuki, T. *J. Am. Chem. Soc.* **2010**, *132*, 5886.

(11) Spek, A. L. *J. Appl. Crystallogr.* **2003**, *36*, 7.

(12) (a) Rajca, A.; Miyasaka, M.; Pink, M.; Wang, H.; Rajca, S. *J. Am. Chem. Soc.* **2004**, *126*, 15211. (b) Dietrich-Buchecker, C.; Rapenne, G.; Sauvage, J.-P.; De Cian, A.; Fischer, J. *Chem.—Eur. J.* **1999**, *5*, 1432.

(13) Accetta, A.; Corradini, R.; Marchelli, R. *Top. Curr. Chem.* **2011**, *300*, 175.

(14) Preliminary X-ray analysis of a single crystal obtained by slow evaporation of a solution of **1a** and Ala showed that it is isostructural to **1a**, in which the Cl anions bound to Zn ions are not replaced by Ala. It is likely that the ligand displacement mechanism<sup>13</sup> might not be responsible for the fluorescence enhancement, although it could not be excluded absolutely.

(15) (a) Soloshonok, V. A.; Ellis, T. K.; Ueki, H.; Ono, T. *J. Am. Chem. Soc.* **2009**, *131*, 7208. (b) Ryu, D.; Park, E.; Kim, D.-S.; Yan, S.; Lee, J. Y.; Chang, B.-Y.; Ahn, K. H. *J. Am. Chem. Soc.* **2008**, *130*, 2394.

(16) (a) Liu, Y.; Xuan, W.; Cui, Y. *Adv. Mater.* **2010**, *22*, 4112. (b) Xiong, R.; You, X.; Abrahams, B. F.; Xue, Z.; Che, C. *Angew. Chem., Int. Ed.* **2001**, *40*, 4422. (c) Li, G.; Yu, W.; Cui, Y. *J. Am. Chem. Soc.* **2008**, *130*, 4582. (d) Nuzhdin, A. L.; Dybtsev, D. N.; Bryliakov, K. P.; Talsi, E. P.; Fedin, V. P. *J. Am. Chem. Soc.* **2007**, *129*, 12958. (e) Bradshaw, D.; Prior, T. J.; Cussen, E. J.; Claridge, J. B.; Rosseinsky, M. J. *J. Am. Chem. Soc.* **2004**, *126*, 6106. (f) Vaidhyanathan, R.; Bradshaw, D.; Rebilly, J.; Barrio, J. P.; Gould, J. A.; Berry, N. G.; Rosseinsky, M. J. *Angew. Chem., Int. Ed.* **2006**, *45*, 6495. (g) Kaczorowski, T.; Justyniak, I.; Lipiska, T.; Lipkowski, J.; Lewiski, J. *J. Am. Chem. Soc.* **2009**, *131*, 5393. (h) Seo, J. S.; Whang, D.; Lee, H.; Jun, S. I.; Oh, J.; Jeon, Y. J.; Kim, K. *Nature* **2000**, *404*, 982. (i) Evans, O. R.; Ngo, H. L.; Lin, W. *J. Am. Chem. Soc.* **2001**, *123*, 10395. (j) Xiang, S.; Zhang, Z.; Zhao, C.; Hong, K.; Zhao, X.; Ding, D.; Xie, M.; Wu, C.; Das, M. C.; Gill, R.; Thomas, K. M.; Chen, B. *Nat. Commun.* **2011**, *2*, 204.